Coherent neutron scattering study of confined water in nafion

F. Sacchetti,[1] A. Orecchini,[1,2] A. Cunsolo,[3] F. Formisano,[4] and C. Petrillo[1]
[1]*Dipartimento di Fisica, Università di Perugia, I-06123 Perugia, Italy*
and CNR-INFM CRS-Soft c/o Università di Roma "La Sapienza," I-00185 Roma, Italy
[2]*Institut Laue-Langevin, F-38042 Grenoble, France*
[3]*Argonne National Laboratory, Lemont, Illinois 60439, USA*
[4]*CNR-INFM CRS-Soft, OGG c/o Institut Laue-Langevin, F-38042 Grenoble, France*
(Received 13 December 2008; revised manuscript received 16 May 2009; published 20 July 2009)

The vibrational dynamics of water molecules confined inside the cavities of a nafion membrane has been investigated exploiting the experimental technique of Brillouin neutron scattering to cover two different kinematic regions. Despite the complexity of the experiments, the inelastic data show unambiguously that confined water still sustains collective modes, although the mode lifetime is affected by a larger damping than in bulk water. The collective-mode velocity (3040 m/s) is found to be much higher than the hydrodynamic value (1320 m/s), such as in the case of bulk water. The structure of the inelastic peaks is consistent with a complex picture where normal vibrational modes of a water droplet coexist with the collective excitation. In addition, no evidence of the second nondispersive excitation at $\simeq 6$ meV observed in bulk water is seen in the present experiment. Finally, the analysis of the inelastic integrated intensities suggests that the anomalous trend observed in bulk water at low-momentum transfers disappears under geometrical confinement.

DOI: 10.1103/PhysRevB.80.024306 PACS number(s): 33.15.−e, 37.30.+i, 61.25.Em, 63.50.−x

I. INTRODUCTION

The study of the microscopic dynamics of liquid water still represents a challenging subject and plays a unique role for a comprehensive understanding of the molecular interactions which drive the peculiar thermodynamic behavior of this complex liquid.[1] Several investigations on both collective and self-dynamics of bulk water, aimed at a complete mapping of the density-density correlation function, were carried out by meV resolution inelastic scattering of both neutrons[2–5] and x rays.[6,7] Evidence for a significant link between the water dynamical features and the extended hydrogen-bond network was reported, together with a complex temperature and pressure dependence of the collective excitations.[4,5,7,8] However, despite the thorough experimental investigations and the parallel invaluable aid of numerical computations,[9] definitive conclusions about the influence of the hydrogen-bond network on the dynamics of water cannot be drawn. This specific point can be brought to focus by a series of tailored dynamical studies on samples characterized by a partially broken network such as, for instance, interfacial water in systems with geometrical confinement.

So far, experimental investigations of confined water dynamics were mostly restricted to measurements of the proton self-correlation function by incoherent neutron scattering in few selected systems.[10] The overall emerging picture is consistent with a splitting of the diffusive processes over two well-separate time scales and suggests that the interactions with the confining substrate remarkably slow down the diffusive motions of interfacial water, while promoting the diffusive flow in bulk water. These single-particle effects are supposedly enhanced when the confining cavity size is on the nm scale, that is, a scale matching the thickness of interfacial water layers. A similar enhancing effect could be conjectured for *coherent* collective excitations in water. Indeed, the propagation velocity of the collective modes in water is strongly wavevector dependent and it changes from some 1320 m/s (normal sound) in the MHz range to more than 3000 m/s (fast sound) in the THz range. In Fig. 1 the plot of the dispersion relation of the energy associated to the collective mode shows that the transition from normal to fast sound develops at exchanged wavevector $Q_c \sim 0.3$ Å^{-1}, which corresponds to an associated wavelength $\lambda_c \sim 20$ Å. According to Refs. 4 and 7, this anomaly in water could reflect a coupling of the collective dynamics to the structural arrangement of the hydrogen-bond network that develops over a similar range. The presence of a peak at about 6 meV in the density of states, also reported in Fig. 1, indicates that

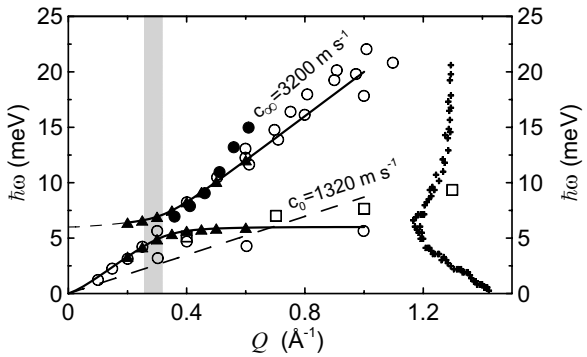

FIG. 1. Summary of the excitation energies observed in water at room temperature by inelastic neutron scattering experiments (dots from Ref. 2 and triangles from Refs. 3 and 4) and by inelastic x-ray scattering experiments (circles from Ref. 6 and squares from Ref. 7). The solid lines are the dispersion relations provided by the model of Ref. 4. The long-dashed line is the hydrodynamic sound (c_0=1320 ms^{-1}) and the curve with crosses on the right is the experimental density of states of light water measured in Ref. 11 and shown over the same energy scale. c_∞=3200 ms^{-1} is the velocity associated to the fast sound velocity and the shaded area shows the transition region around $Q_c \sim 0.3$ Å^{-1}.

additional modes are present in this lower-energy range and it is suggested to be related with the interaction model described in Refs. 3 and 4. On extending this picture to confined water, one could expect visible effects on the collective excitations and their anomalous dispersion when the typical size of water pools inside the confining media gets close to λ_c.

The description of the dynamic-response function of a highly nonhomogeneous system such as confined water could also be achieved by numerical approaches such as, for instance, in the case of protein hydration water.[12] Nonetheless, analytical approaches are very important both to guide experimental and numerical investigations and to provide overall descriptions of the physical principles governing the system. A hydrodynamic-based theoretical model was developed in Ref. 13 to describe the dynamic structure factor of a small spherical liquid droplet. The model predicts that, besides the expected vibrational normal modes of the droplet, hydrodynamic collective modes also exist and propagate inside the droplet. Experimental observations of these excitations are scarce, although evidence for droplet modes developing in the meV region was reported in a recent THz spectroscopy experiment on inverse micelles.[14]

Here we report on a neutron inelastic scattering study aimed at isolating the dynamic response of heavy water confined inside a nafion membrane. Nafion is a perfluorosulfonic polymer membrane characterized by a hydrophobic fluorocarbon backbone and hydrophilic sulfonic acid groups.[15] Thanks to the capability of absorbing large quantities of water, the nafion membrane has been suggested as an optimal candidate for a wide range of device applications.[16–18] Upon hydration, the hydrophilic clusters are saturated by water that appears to be confined in almost spherical cavities with 40 Å average diameter.[15,19,20] With increasing the water content, percolation through the nafion pores can occur, possibly resulting in a network of water cylinders connecting the cavities.[21,22] Water confinement in nafion has been the subject of several investigations, although mostly of structural kind. At present, despite the large number of experiments aimed at determining the average space distribution and shape of the water droplets in nafion,[15,19,22] the measurements do not provide a unified picture and a number of different structural models have been proposed to interpret the transport data. As to atomic-scale dynamics, the only available investigations are the few single-molecule diffusion studies reported and discussed in Ref. 10 and the more recent temperature-dependent quasielastic neutron scattering study of Ref. 23. To our best knowledge no other experiment devoted to the *coherent* collective dynamics of confined water exists apart from that performed on hydrated powders of C-phycocyanin protein[24] where, however, the separation of water and protein contributions was not attempted and only qualitative results could be obtained.

The nafion membrane with the characteristic 40 Å size of its pores offers a good match to the value of the wavelength λ_c at room temperature and represents an ideal system to study the effects of nanoscale confinement on the coherent collective dynamics of water. We mention that the propagation of elementary excitations in quantum (^{4}He) (Ref. 25) and nonclassical (D_2) (Ref. 26) liquids confined in porous media has been far more investigated than the case of a confined prototype hydrogen-bonding system such as water.

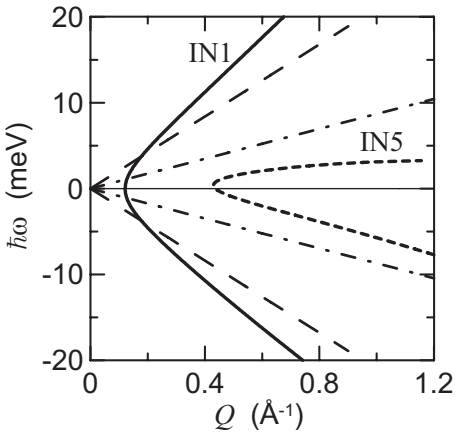

FIG. 2. Dynamic range accessible to the two experiments. The region inside the full line is accessible to the IN1 experiment with 2.3 meV resolution. The region inside the short-dashed line is also accessible to the IN5 experiment with 0.12 meV resolution. The long-dashed line is the fast sound dispersion in bulk water (Refs. 4 and 7) and is visible to the IN1 experiment only. The dispersion of the hydrodynamic sound (1320 m/s) is also reported as a dot-dashed line. Even this much smaller sound velocity is not visible by the IN5 experiment.

II. EXPERIMENT AND DATA TREATMENT

To fully characterize the dynamic response of heavy water confined in the nafion membrane, two inelastic neutron scattering experiments were carried out at room temperature at the high-flux reactor of the Institute Laue Langevin (ILL) in Grenoble (France). The first experiment on the three-axis spectrometer IN1, equipped with the high-resolution Cu(331) monochromator and the Cu(400) analyzer in conjunction with tight collimations $(25',20',20',30')$, was characterized by a fixed final neutron energy equal to 100 meV and an elastic energy resolution of 2.3 meV. Although this is too broad a resolution to properly resolve the droplet normal modes, improving it would severely limit the dynamic range, which has instead to be kept wide enough to detect possible collective excitations usually propagating at higher energies. To access the energy region where droplet modes could develop, the second experiment was performed on the time-of-flight spectrometer IN5 with a selected incoming neutron energy of 3.27 meV and an energy resolution of 0.12 meV. In Fig. 2, an inspection of the dynamic ranges accessible to the two experiments clearly shows that water collective modes can be measured only by the high-energy and broad-resolution configuration of IN1, while the low-energy and high-resolution setup of IN5 enables to investigate the low-lying droplet modes.

The sample was a standard nafion N112 membrane (E. I. DuPont Co.), which was cleaned and pretreated by immersion into 99.9% pure boiling D_2O for one hour and then dried under vacuum. Two samples were employed in the IN1 experiment: a first one made of 18 g of dry membrane kept

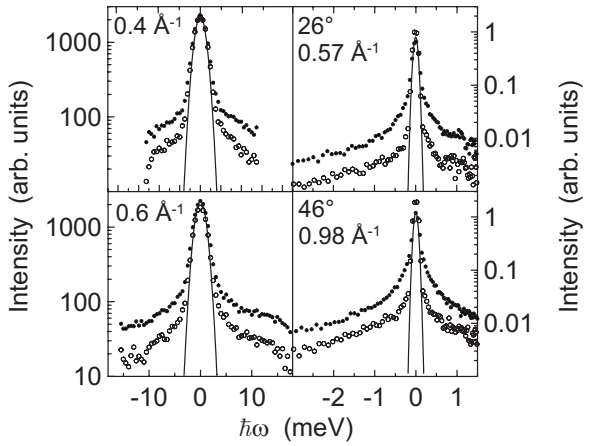

FIG. 3. Inelastic spectra versus exchanged energy at two selected wavevector transfers as obtained by IN1 (left panel) and IN5 (right panel). The data of the wet (dots) and dry (circles) membrane are plotted in log scale after empty cell and background subtraction. The full line is the resolution function normalized to the wet sample data. For the constant-angle spectra of IN5, the corresponding elastic Q values are also quoted.

inside a flat vacuum-tight Al container (80 mm×40 mm ×8 mm) and a second one where ~10 g of D_2O, i.e., a quantity slightly exceeding the maximum absorbable amount, were poured in the container onto the dry membrane. A 4-mm-high hollow Cd spacer was inserted at the bottom of the cell to enable water in excess, in the case of the second sample, to accumulate there. This expedient ensured the thermal equilibrium of the wet membrane with heavy-water vapor to be maintained during the measurements. Inelastic scans at six values of wavevector transfers, namely, $Q=0.25, 0.3, 0.4, 0.5, 0.6, 0.7$ Å^{-1}, were collected for both the samples, the empty container, and the environmental background. The elastic energy resolution for the adopted IN1 configuration was measured on a vanadium standard. A full width at half maximum equal to 2.3 meV, as anticipated, resulted from the Gaussian best fit of the vanadium spectrum. In the IN5 experiment, the same strategy was adopted: about 1.5 g of dry nafion membrane, to which ~1 g of heavy water was added later, were contained into the hollow between two coaxial Al cylinders (15 mm outer diameter, 13 mm inner diameter, 50 mm height). Constant-angle spectra were collected between 20° and 120° for both the samples, the empty container, and the environmental background. As an example, Fig. 3 shows typical experimental spectra of the wet and dry membrane, after empty cell and background subtraction, collected on IN1 (left panel) and IN5 (right panel).

A proper data treatment was developed to correct the data for unwanted contributions, such as the ordinary empty cell and background, but mostly to obtain the dynamic response function of confined water out of the data measured on dry and wet nafion. Extracting the sole water contribution in a nanometer confined system is an *a priori* complex task due to the coupling of the density-fluctuation spectrum with specific features of the confining substrate such as geometry and size of the cavities or properties of the substrate material. Further, there is the intrinsic difficulty of properly identifying the dynamic contribution of the membrane which has to be subtracted, although it changes upon hydration. In fact, the experimental spectra of the dry sample cannot be simply taken as a straightforward measurement of the membrane scattering contribution in the wet sample. To minimize these effects, the reduction procedure here proposed exploits the measured intensity data at most and is based upon assumptions supported by trends otherwise apparent in the experimental data themselves. Quite generally, the dynamic structure factor $S(Q,\omega)$, which the measured intensity is proportional to, can be decomposed into the sum of quasielastic (about $\omega=0$), $S^{qe}(Q,\omega)$, and inelastic, $S^{in}(Q,\omega)$, terms. Indeed, Fig. 3 shows that the experimental spectra are made up of a rather broad quasielastic contribution that is better characterized by the IN5 measurements, and of purely inelastic tails whose features are clearly apparent over the extended energy range of the IN1 scans. Further, we observe that the inelastic tails are consistently more intense in the wet than in the dry sample. The key point of the proposed analysis is the proper identification of the effect brought about by the presence of water on the quasielastic and purely inelastic components of the measured spectra.

We started assuming that the wet nafion membrane can be modeled as a sample made of N_{nafion} nafion scattering units, characterized by scattering length b_{nafion} and density n_{nafion}, and N_{water} water molecules distributed within the membrane pores, whose shape is not *a priori* specified, with scattering length b_{water} and density n_{water}. For such a system, the dynamic structure factor is decomposed as $S_{wet}(Q,\omega) = S^{qe}_{wet}(Q,\omega) + S^{in}_{wet}(Q,\omega)$ and the quasielastic intensity, $I^{qe}_{wet}(Q,\omega)$, can be written as

$$I^{qe}_{wet}(Q,\omega) \propto S^{qe}_{wet}(Q,\omega) \otimes R(\omega) = [S^{qe,coh}_{wet}(Q,\omega) + S^{qe,inc}_{wet}(Q,\omega) + S^{SANS}_{wet}(Q,\omega)] \otimes R(\omega), \quad (1)$$

where $R(\omega)$ is the instrumental resolution function, $S^{qe,coh}_{wet}(Q,\omega)$ is the coherent quasielastic contribution brought about by all the intermolecular correlations, and $S^{qe,inc}_{wet}(Q,\omega)$ is the incoherent counterpart. $S^{SANS}_{wet}(Q,\omega)$ is a small-angle term that originates from the change in average scattering density between water and nafion and is given by

$$S^{SANS}_{wet}(Q,\omega) = |(\rho_{\text{water}} - \rho_{\text{nafion}}) f(Q)|^2 \delta(\omega),$$

where $\rho=nb$ is the scattering density and $f(Q)$ is a form factor that accounts for the shape of the water-filled pores giving rise to small-angle scattering contributions. Here, it is assumed that the small-angle contribution is characterized by quite a sharp energy dependence in comparison with the rather broad energy resolution of both the experiments. As to the purely inelastic contribution, the response is approximated by the sum of nafion and water inelastic contributions separately, that is,

$$I^{in}_{wet}(Q,\omega) \propto S^{in}_{wet}(Q,\omega) \otimes R(\omega) = [S^{in}_{\text{nafion}}(Q,\omega) + S^{in}_{\text{water}}(Q,\omega)] \otimes R(\omega). \quad (2)$$

Here the assumption is made that the nafion-water interfacial term gives a negligible contribution. Actually, this is not a

statement of general validity for two-component systems. However the collective modes observed in hydrated nafion, as well as in pure water, show a sizeable damping and a correspondingly short mean-free path. Inelastic correlations are thus contributed only by atomic pairs closer than the mean-free path. For water-water (nafion-nafion) contributions, such close-enough atomic pairs are spread all over the water (nafion) volume. On the contrary, they are limited to a thin layer around the water droplets in the case of the mixed water-nafion contribution. For such geometrical reasons, the nafion-water interfacial term is expected to be significantly reduced. To support this qualitative guess, we estimated the order of magnitude of the water-water, water-nafion, and nafion-nafion inelastic contributions by a numerical model which assumes the presence of damped waves traveling through the water droplets and in the nafion membrane. For simplicity, the water droplets were considered spherical with a radius of 2 nm and dispersed into the nafion membrane. As a result, water-nafion cross correlations turned out to be about one order of magnitude smaller than the water-water and nafion-nafion coherent correlations in the whole range of investigated wavevector transfer. We note also that the dominating inelastic terms $S^{in}_{\mathrm{nafion}}(Q,\omega)$ and $S^{in}_{\mathrm{water}}(Q,\omega)$ contain their own coherent and incoherent contributions. Nevertheless, the atomic species composing the nafion membrane (C, O, F, and S) have negligibly small incoherent cross sections. Heavy water can instead bear significant incoherent scattering due to the cross section of deuterium atoms. However, the investigations of Refs. 3 and 4 have shown that, in the low-momentum transfer range under study, heavy-water incoherent scattering is primarily confined to the quasielastic region with negligible contributions to the inelastic range.

The companion relationships for the intensity measured on the dry nafion membrane are

$$I^{qe}_{dry}(Q,\omega) \propto S^{qe}_{dry}(Q,\omega) \otimes R(\omega) = [S^{qe,coh}_{dry}(Q,\omega) + S^{qe,inc}_{dry}(Q,\omega) + S^{SANS}_{dry}(Q,\omega)] \otimes R(\omega), \tag{3}$$

$$I^{in}_{dry}(Q,\omega) \propto S^{in}_{dry}(Q,\omega) \otimes R(\omega) = S^{in}_{\mathrm{nafion}}(Q,\omega) \otimes R(\omega), \tag{4}$$

where

$$S^{SANS}_{dry}(Q,\omega) = |\rho_{\mathrm{nafion}} f(Q)|^2 \delta(\omega).$$

This set of equations contains the major approximation that upon hydration of the cavities the dynamic response of nafion does not change but for the small-angle term (SANS) that depends on the contrast between the bulk membrane and the medium filling the pores. Considering the fairly small inelastic scattering of the dry membrane, this approximation is safe for this term. From the above set of equations, the dynamic response of the sole water confined into the cavities is obtained, that is,

$$S_{\mathrm{water}}(Q,\omega) = S_{wet}(Q,\omega) - S_{dry}(Q,\omega) - [S^{SANS}_{wet}(Q,\omega) - S^{SANS}_{dry}(Q,\omega)]. \tag{5}$$

Introducing the contrast factor

$$R_c = \frac{(\rho_{\mathrm{nafion}} - \rho_{\mathrm{water}})^2}{\rho^2_{\mathrm{nafion}}},$$

it follows

$$S^{SANS}_{wet}(Q,\omega) = R_c S^{SANS}_{dry}(Q,\omega).$$

The outlined approach can be applied to the measured intensities of the dry and the wet samples to obtain the intensity contribution of the sole water, that is,

$$I_{\mathrm{water}}(Q,\omega) = I^{exp}_{wet}(Q,\omega) - T_{\mathrm{water}}[I^{exp}_{dry}(Q,\omega) - (1-R_c) I^{SANS}_{dry}(Q,\omega)]. \tag{6}$$

T_{water} is the transmission of water equal to 0.79 and 0.90 for the IN1 and the IN5 experiments, respectively, resulting from the samples scattering density and geometry. The scattering densities ρ contained in R_c are calculated according to the chemical compositions of nafion and water using the known densities n and scattering lengths b which yield $\rho_{\mathrm{nafion}}=4.5\times10^{10}$ cm^{-2} and $\rho_{\mathrm{water}}=6.3\times10^{10}$ cm^{-2}. Equation (6) contains the unknown small-angle intensity $I^{SANS}_{dry}(Q,\omega)$ that has to be subtracted from the experimental data. A possible approach could be that of calculating the form factor $f(Q)$ from a structural model of the nafion membrane to provide an estimate of $I^{SANS}_{dry}(Q,\omega)$. We preferred to avoid this procedure and to make use of approximations supported by the trends in the experimental data. Actually, Eq. (3) shows that the SANS term can be obtained from the quasielastic intensity by the subtraction of the quasielastic coherent and incoherent contributions. These two contributions can be safely considered as Q independent over the wavevector range of the present experiments ($0.25<Q<1$ Å^{-1}), whereas the SANS term is expected to rise at low Q ($Q<Q_0=0.4$ Å^{-1}) and to be negligible at higher Q values. Therefore, $I^{SANS}_{dry}(Q,\omega)$ can be evaluated by subtracting the large-Q limit of the quasielastic intensity, which amounts to the sum of coherent and incoherent contributions, from the quasielastic intensity itself, i.e.,

$$I^{SANS}_{dry}(Q,\omega) = I^{qe}_{dry}(Q,\omega) - [I^{qe}_{dry}(Q,\omega)]_{Q>Q_0}. \tag{7}$$

To draw out the signal of confined water by applying the proposed approach, it is clear that the term $I^{qe}_{dry}(Q,\omega)$ is finally needed.

To first ascertain the validity of the approximations here used, we started with the separate analysis of both the dry, $I^{exp}_{dry}(Q,\omega)$, and the wet, $I^{exp}_{wet}(Q,\omega)$, intensities measured on IN1 with the only purpose of preliminarily analyzing the Q dependences of the energy-integrated quasielastic and inelastic intensities. Therefore, after standard empty cell and background subtraction, both the intensities were fitted to the simple model function

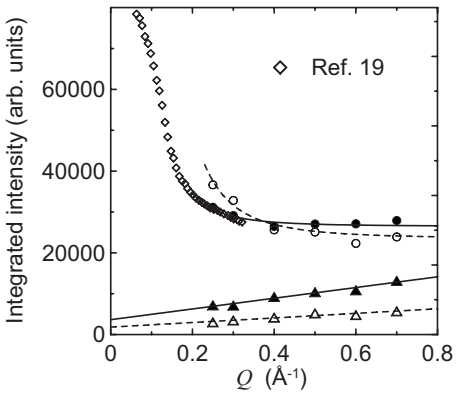

FIG. 4. Q dependence of the energy-integrated Lorentzian (dots) and DHO (triangles) curves best fitting the quasielastic and inelastic intensities, respectively [see Eq. (8)]. Full symbols: wet membrane. Open symbols: dry membrane. Diamonds: small-angle static structure factor $S(Q)$ of wet nafion membrane, as measured in Ref. 19. Lines are guides to the eye.

$$I_{mod}(Q,\omega) = I^{qe}_{mod}(Q,\omega) + I^{in}_{mod}(Q,\omega) = \left\{ \frac{\beta\omega}{1-\exp(-\beta\omega)} \frac{a_{qe}(Q)}{\pi} \frac{\Gamma_{qe}(Q)}{\omega^2+\Gamma^2_{qe}(Q)} + a_{in}(Q) \times [n(\omega)+1] \frac{\Gamma_{in}(Q)\omega}{[\omega^2-\omega^2_{in}(Q)]^2+\Gamma^2_{in}(Q)} \right\} \otimes R(\omega), \tag{8}$$

with the Lorentzian function describing the quasielastic contribution, the damped harmonic-oscillator (DHO) term accounting for the purely inelastic features of the spectra, and $n(\omega)$ standing for the Bose factor. The free parameters of the fit were the amplitudes of the quasielastic and inelastic components $a_{qe}(Q)$ and $a_{in}(Q)$, respectively, the corresponding widths $\Gamma_{qe}(Q)$ and $\Gamma_{in}(Q)$, and the energy associated to the DHO inelastic mode $\hbar\omega_{in}(Q)$. The overall quality of the fit was adequate enough to produce energy-integrated intensities out of the best-fitting analytical curves, namely, the Lorentzian and the DHO functions. The results are summarized in Fig. 4 where an almost constant behavior with a slight increase at the lowest Q's is observed for the integrated quasielastic intensity, opposite to the monotonic linear growth that characterizes the inelastic term. The *excess* of quasielastic intensity at low Q can be taken as a fingerprint of the SANS features arising from nanometer confinement, whereas the regular trend of the inelastic intensity suggests this term being weakly affected by confinement. We also note that the integrated inelastic intensity is significantly smaller in the dry than in the wet membrane, while the low-Q increase in the quasielastic contribution is larger in the dry membrane, which is an expected effect due to the higher contrast. These findings support the assumption upon which the proposed data analysis is based, namely, that wetting of the membrane affects the quasielastic component of the spectrum through the different contrast coefficient of the SANS term only. This straightforward, not sophisticated but reliable analysis of the IN1 data, served the purpose of providing a set of clear results to ground the dry-from-wet subtraction procedure on (see Eq. (6)). We also mention that trends similar to those shown in Fig. 4 were found for the integrated intensities resulting from fitting the IN5 data with the same model functions (Eq. (8)).

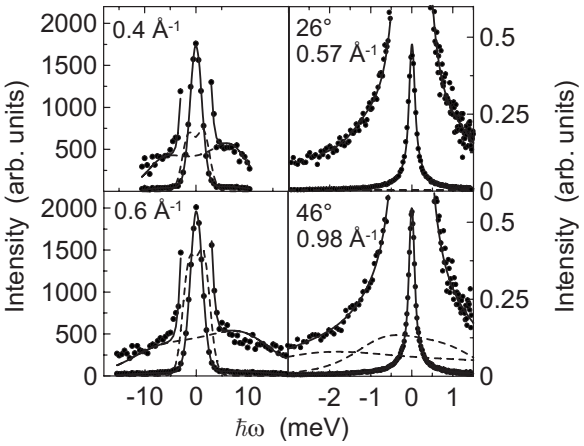

FIG. 5. Experimental dynamic response of confined water in nafion at two chosen wavevector-transfer values, as obtained by IN1 (left panel) and IN5 (right panel). The full line is the best-fitting curve resulting from the model described in the text (see Eq. (9)) while the dashed lines are the DHOs describing the inelastic contributions. To point out the good quality of the fits on both the elastic peak and the inelastic tails of the spectra, the data and the modeling curves are plotted on both full and expanded scale, the expansion factor amounting to 10 and 20 for the IN1 and IN5 data, respectively. For the constant-angle spectra of IN5, the corresponding elastic Q value is also quoted.

With Eq. (6) also supported by the integrated intensities analysis, we applied the proposed reduction procedure where all the quantities are provided by measured intensities but the quasielastic dry term that, although contributing to the experimental spectra, cannot be isolated in a single experiment. The most-suited account for this term is then given by the corresponding model function $I^{qe}_{mod}(Q,\omega)$ best fitting the dry-sample data.

Typical results for the confined-water spectra are shown in Fig. 5 for both IN1 and IN5 experiments. The spectra obtained from the IN1 data (left panel) show a clear inelastic signal that extends over a rather wide energy range while the central quasielastic peak is broad and featureless. More detailed information about the low-energy region of the spectra is provided by the high-resolution data of IN5 (right panel), which reveal that the featureless quasielastic signal observed on IN1 is actually structured and can be decomposed into the sum of a much more narrow intense quasielastic peak and some low-energy inelastic shoulders. We also note that, since the water droplets are not monodisperse but are characterized by a broad size and shape distribution, rather featureless inelastic tails are expected as, indeed, observed in the IN5 experiment.

III. DATA ANALYSIS AND DISCUSSION

To interpret the so obtained spectra of confined water, we resorted to an empiric model founded upon the results of the

theoretical approach of Ref. 13. There, the *coherent* scattering function was calculated for density fluctuations in spherical fluid particles. Assuming that the water-filled cavities in nafion can be reasonably well approximated by spherical fluid droplets not diffusing within the matrix, a model coherent dynamic structure factor can be obtained from Eqs. 3.16 and 3.18 of Ref. 13 by setting to zero the there-defined parameter "Γ", that is proportional to the diffusion constant of the massive fluid droplets. Those equations are then reduced to the following form:

$$S_{\mathrm{drop}}(Q,\omega) \propto \sum_j G_j(Q) \frac{\theta_j^4 c^2 \eta^2}{[\omega^2 - (\theta_j c)^2]^2 + (\omega \theta_j^2 \eta)^2},$$

where $S_{\mathrm{drop}}(Q,\omega)$ is the droplet dynamic structure factor, $G_j(Q)$ is the weight function given in Ref. 13, θ_j is a momentum obtained from the boundary conditions assumed at the droplet surface, c is the sound velocity, and η is the kinematic viscosity. The response of the droplet, thus, is a series of DHOs centered at Q-independent frequencies $\omega_j = \theta_j c$ and with $\Gamma_j = \theta_j^2 \eta$ as damping factor, a form which accounts for the normal modes of the spherical fluid particles. On increasing the momentum transfer, since $G_j(Q)$ is peaked when $\theta_j \simeq Q$, an additional DHO is also present with $\omega_j = cQ$ and $\Gamma_j = \eta Q^2$. According to Ref. 13, this form is only appropriate in the hydrodynamic limit, that is, in the continuum region where the mode wavelength is much larger than the intermolecular distances into play. To extend such an approach beyond the hydrodynamic limit and adopt it as a guide to interpret the higher-frequency data of the present study, the response function of the jth DHO can be defined as $\Gamma_j(Q)\omega/[(\omega^2 - \omega_j(Q)^2)^2 + (\Gamma_j(Q)\omega)^2]$, where $\hbar\omega_j(Q)$ is the DHO characteristic energy and $\hbar\Gamma_j(Q)$ is the corresponding damping factor. Here, $\omega_j(Q)$ and $\Gamma_j(Q)$ are no more restricted to the hydrodynamic form and can instead assume a larger variety of Q dependences. The so-obtained dynamic structure factor is thus a sum of DHOs which can describe both normal droplet modes of constant frequency and propagating density fluctuations with a proper dispersion curve $\omega_j(Q)$.

To take into account the quasielastic contribution observed in the experimental data, a sharp Lorentzian function was further added to the sum of the DHOs. Such quasielastic contribution, absent in the original model,[13] is indeed expected to be present because of the non-negligible incoherent scattering of heavy water, as discussed in the previous section. The complete model was used to simultaneously fit *all* the spectra from both the IN1 and the IN5 experiment, namely, the convolution of the model function with the resolution function as appropriate to IN1 and IN5 was fitted to the whole available experimental data set. As a result of several trials, the minimum number of DHOs necessary to execute a meaningful fit of all the data turned out to be one high-frequency DHO and two further DHOs at low frequency. Therefore the model curve best fitting the dynamic structure factor of confined water is

$$S^{mod}_{\mathrm{water}}(Q,\omega) = \frac{\beta\omega}{1-\exp(-\beta\omega)} \frac{A_L(Q)}{\pi} \frac{\Gamma_L(Q)}{\omega^2 + \Gamma_L^2(Q)} + \sum_{j=1}^{3} A_j(Q) \times [n(\omega)+1] \frac{\Gamma_j(Q)\omega}{[\omega^2 - \omega_j^2(Q)]^2 + \Gamma_j^2(Q)}. \quad (9)$$

The quality of the fit, with the 11 free parameters $A_L(Q)$ and $\Gamma_L(Q)$, and $A_j(Q)$, $\Gamma_j(Q)$, and $\omega_j(Q)$ with $j=1,2,3$ was very good at all Q values and for both sets of experiments at the same time, as it is apparent in Fig. 5.

The reliability of the model of Eq. (9), based on the approach of Ref. 13, was assessed against different trial functions by carrying out a statistical analysis of the results. The simplest model, suited for the IN1 spectra only, was given by the sum of a broad Lorentzian curve and just one high-frequency DHO. Although the overall quality of this fit was reasonably good, the quasielastic peak was found to have a Q-independent width of 2.7 meV that is definitely not compatible with the IN5 data. It is thus clear that the deeper nature of such a broad and unphysical quasielastic component can only be understood by a closer inspection of the IN5 spectra.

To proceed with the analysis of the IN5 data, we first show that they contain such an amount of information that can only be satisfactorily described by a multicomponent fitting function. To this end, we tried to fit the IN5 data with just one single quasielastic peak plus a constant. By such a simple model it was not possible to produce an acceptable fit, the best obtainable reduced χ^2 amounting to about 6. It is then clear that a more complex model must be used to correctly reproduce the data. As an alternative to the DHO model of Eq. (9), the IN5 data were thus fitted by a sum of Lorentzian functions. Three components were necessary to achieve a fit quality comparable to that obtained by the model of Eq. (9) (see below for a safe approach to the best number of components to be used in the fit). We shall remark that the three Lorentzian functions here play the role of the sharp Lorentzian peak plus the two low-frequency DHOs in Eq. (9). The third high-frequency DHO is indeed out of the energy window of IN5 and is only visible by IN1. As a result of the multiLorentzian fit on the IN5 data, a rather unphysical Q-independent width of all components was again obtained. Nevertheless, this fit is completely compatible with the IN1 data in that it can correctly reproduce the large quasielastic contribution observed in the IN1 energy window.

For a safer and grounded choice of the most appropriate modeling function, the IN1 and IN5 spectra were further exploited to carry out a quantitative statistical analysis of the two models. This analysis aims at deriving a ratio between the posterior probabilities for the two models, given the experimental data, on the basis of the Bayesian approach outlined by Sivia[27] and successfully applied to a neutron scattering experiment in Ref. 28. The posterior probability $P(H|D,I)$ of the hypothesis H conditioned by the data D and by the possible previous knowledge I is given by

$$P(H|D,I) \propto P(D|H,I)P(H|I),$$

where the probability of the data, given the hypothesis H, can be reasonably taken proportional to the likelihood func-

tion of the data once the fit to the model derived from H is performed.[27,28] The prior probability $P(H|I)$ can be either determined from the noninformative single-Lorentzian fit given above[28] or by assuming that the ratio $P(H_{\mathrm{DHO}}|I)/P(H_{\mathrm{LOR}}|I)$ is equal to unity, where H_{DHO} and H_{LOR} correspond to the DHO model and the three-Lorentzian model, respectively. The same approach can be used to determine the best-suited number of components[28] given H_{DHO} or H_{LOR}. As a first result of such analysis, we found out that for both models, a minimum of three components is necessary to reach a plateau for the posterior probability. In addition, the ratio of the posterior probabilities $P(H_{\mathrm{DHO}}|D,I)/P(H_{\mathrm{LOR}}|D,I)$ resulted to be about 10 at all Q values, if $P(H_{\mathrm{DHO}}|I)/P(H_{\mathrm{LOR}}|I)$ is assumed to be unity. The DHO model, which assumes the presence of the droplet modes, is therefore strongly favored by the Bayesian analysis. In view of this result, the DHO model of Eq. (9) is considered in the following as the basis for further discussion.

The wavevector dependence of the best-fit DHO energies $\hbar\omega_j$ is plotted in Fig. 6 and compared with companion data in bulk water taken from the literature. The first clear conclusion one can draw is that a fast collective mode (dots) is present in the confined-water droplets, similar to bulk water. Indeed, a linear fit to this dispersion curve provides a velocity of 20 meV Å=3040 m/s, much higher than the hydrodynamic sound velocity in heavy water at room temperature (8.7 meV Å=1320 m/s). This first finding demonstrates that confinement does not suppress the high-energy collective mode which is, on the contrary, characterized by a frequency and a dispersion resembling those of fast sound in bulk water.[4,7] A rather similar conclusion was also drawn in previous investigations on hydrated proteins.[12,24,29] The similarities with bulk water, however, are limited to the fast sound: indeed the best fit of the present spectra does not require the introduction of the second mode observed in bulk water around 6 meV.[4,7] The two additional modes (squares) that are necessary to fit the IN5 spectra and show Q-independent energies of 1.4 and 3.7 meV can instead be attributed to droplet oscillations. Of course, one could speculate about a connection of these two modes with the 6 meV peak observed in bulk water. Since the water molecules are rearranged in the confined configuration, we cannot rule out the possibility that the interaction with the confining medium induces a splitting of the 6 meV mode in two modes of lower frequencies. However it is also important to recall that the 6 meV mode is strongly reduced already in vycor-confined water.[11] Therefore, according to the present model fitting and to previous observations, we believe that the two low-frequency modes can be more reasonably attributed to proper modes of the water droplets.

A second remarkable result, shown in the central panel of Fig. 6, is the fact that the damping factor of the fast collective mode is much larger in nafion-confined water (dots) than in bulk water (circles). The resulting almost-overdamped propagation of the collective mode within the water droplets may be related to the scattering of sound waves from the droplet boundaries. This process is difficult to model since the distribution of water in nafion is quite complex and the microscopic structure is ill defined.[15] However, if the nafion

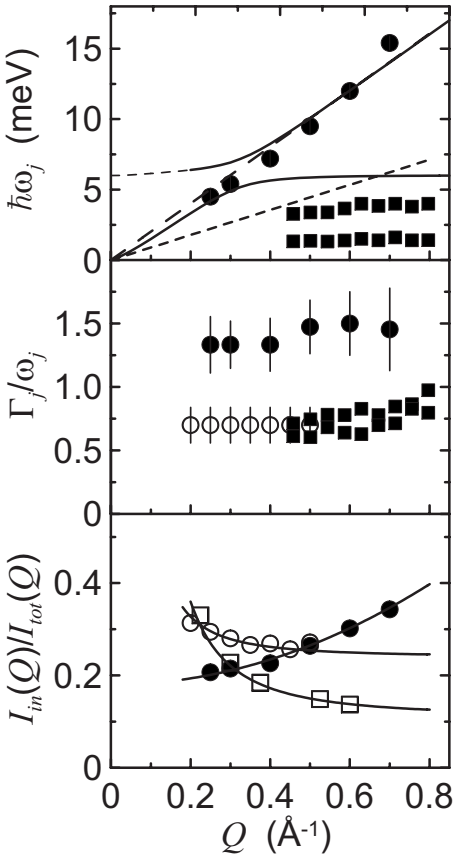

FIG. 6. Upper panel: dispersion relations associated to the collective (dots) and to the droplet (squares) modes. Short-dashed line: linear dispersion relation of the hydrodynamic sound in bulk D_2O. Long-dashed line: linear fit to the collective mode of confined water. Full line: model dispersion relation in bulk water from Ref. 4. Central panel: Γ_j/ω_j ratio of the confined-water collective mode (dots) against the same ratio for bulk D_2O (circles) and of the droplet modes (squares). Lower panel: ratio $I_{in}(Q)/I_{tot}(Q)$ between the inelastic integrated intensity and the total integrated intensity for confined water (dots) and bulk water from neutron scattering (Ref. 4) (circles) and x-ray scattering (Ref. 7) (empty squares) as analyzed in Ref. 4. The full lines are guides to the eyes.

cavities are modeled as spheres of 40 Å diameter, the root-mean-square distance d of two points within the cavity amounts to about 22 Å. On the other hand, the mean-free path l of the collective mode, propagating in three dimension, can be estimated by the relation $l \sim 6c/\Gamma$ and turns out to be on the order of 10 to 20 Å. The reasonable agreement between the estimated values of d and l can support the idea of an increased damping due to the dimensions of the confining cavity. Conversely, it is interesting to observe that both droplet modes (squares) show a Γ_j/ω_j ratio very close to that of fast sound in bulk water. Actually it is not surprising that confinement does not affect the damping factors of droplet normal modes, considering that the damping mechanism of these nonpropagating excitations mainly depends on the viscosity[13] rather than on the characteristic size of the medium.

A comparative analysis of the inelastic integrated intensity of the high-frequency collective mode provides further

insight onto the effect of confinement. The lower panel of Fig. 6 reports the $I_{in}(Q)/I_{tot}(Q)$ ratio of the inelastic integrated intensity to the total integrated intensity for water in nafion (dots), in comparison with the companion data in bulk water from both neutron[4] (circles) and x ray[7] (squares) scattering experiments. Water in nafion follows a rather regular behavior with the intensity ratio decreasing smoothly toward low Q, whereas bulk water shows an anomalous rise. Such peculiarity of bulk water could be related to the known anomalous increase at low Q in the static structure factor,[30] which is observed in the supercooled region. The present findings suggest that confined water in nafion at low wavevector transfers follows a trend more similar to that of a *normal* liquid, where the energy-integrated dynamic structure factor approaches from above a constant limiting value (hydrodynamic limit). Such recovery of the *normal* behavior of the inelastic intensity could be ascribed to the breaking of the hydrogen-bond network caused by confinement.

In conclusion, the study of coherent density fluctuations in small water pools embedded in a nafion membrane enables further understanding of the role of the hydrogen-bond network on the collective dynamics of water. Indeed, we observe that confinement in nafion seems to wipe off the anomalous increase in the inelastic intensity at low Q and the occurrence of a second excitation at 6 meV.[4,7] On the contrary, the propagation velocity of the fast sound observed in bulk water is unaffected by confinement in nafion even though the presence of the droplet boundaries seems to reduce the lifetime of this mode. Finally, we also observe a couple of additional oscillating modes which are attributed to normal vibrations of the water droplet.[13] The damping factor of these droplet oscillations is found to be almost wavevector independent, consistently with the presence of a shape and size distribution of the water droplets, which introduces a fluctuation of the proper frequency of the droplet modes. In further support of the interpretation of the observed low-lying excitations as droplet normal modes, the present results can be compared with those obtained by Terahertz spectroscopy on water confined in nm-sized micelles.[14] In Fig. 7, we plot the surface mode energy of the liquid-water pools vs the pool radius as reported in Ref. 14. The energy of the lowest observed droplet mode in wet nafion (1.4 meV), which is attributed to the average radius of cavities in the nafion membrane (2 nm), is actually in excellent agreement with the results of Ref. 14.

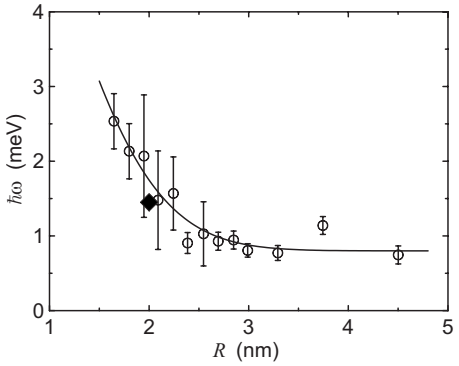

FIG. 7. Surface mode energy of liquid-water droplets as a function of the droplet radius after Ref. 14 (empty circles). The energy of the lowest mode in nafion-confined water here observed is shown for comparison (diamond).

ACKNOWLEDGMENTS

We wish to thank the ILL for providing beam time, along with the local contacts A. Ivanov and H. Mutka for assistance during the experiments on IN1 and IN5, respectively.

[1] The existing literature on water is so large that an exhaustive list cannot be provided herewith. Comprehensive texts of major reference are P. G. Debenedetti, *Metastable Liquids* (Princeton University Press, Princeton, 1996); *Water: A Comprehensive Treatise*, edited by F. Franks (Plenum, New York, 1972), Vol. 1; Updated references on water structure and dynamics can be found in the two reviews: P. Ball, Chem. Rev. (Washington, D.C.) **108**, 74 (2008); B. Bagchi, *ibid.* **105**, 3197 (2005); Further references on confined, supercooled, and glassy water in C. Angell, Science **319**, 582 (2008).

[2] J. Teixeira, M. C. Bellissent-Funel, S. H. Chen, and B. Dorner, Phys. Rev. Lett. **54**, 2681 (1985).

[3] C. Petrillo, F. Sacchetti, B. Dorner, and J.-B. Suck, Phys. Rev. E **62**, 3611 (2000).

[4] F. Sacchetti, J.-B. Suck, C. Petrillo, and B. Dorner, Phys. Rev. E **69**, 061203 (2004), and references therein.

[5] J. Teixeira, M.-C. Bellissent-Funel, S. H. Chen, and A. J. Dianoux, Phys. Rev. A **31**, 1913 (1985); A. Cunsolo, A. Orecchini, C. Petrillo, and F. Sacchetti, J. Chem. Phys. **124**, 084503 (2006), and references therein.

[6] F. Sette, G. Ruocco, M. Krisch, C. Masciovecchio, R. Verbeni, and U. Bergmann, Phys. Rev. Lett. **77**, 83 (1996).

[7] E. Pontecorvo, M. Krisch, A. Cunsolo, G. Monaco, A. Mermet, R. Verbeni, F. Sette, and G. Ruocco, Phys. Rev. E **71**, 011501 (2005), and references therein.

[8] A. Cunsolo, A. Orecchini, C. Petrillo, and F. Sacchetti, J. Phys.: Condens. Matter **19**, 415118 (2007).

[9] F. W. Starr, S. Harrington, F. Sciortino, and H. E. Stanley, Phys. Rev. Lett. **82**, 3629 (1999); F. W. Starr, F. Sciortino, and H. E. Stanley, Phys. Rev. E **60**, 6757 (1999); C. Y. Liao, F. Sciortino, and S. H. Chen, *ibid.* **60**, 6776 (1999).

[10] M.-C. Bellissent-Funel, Eur. Phys. J. E **12**, 83 (2003).

[11] M.-C. Bellissent-Funel, S. H. Chen, and J.-M. Zanotti, Phys. Rev. E **51**, 4558 (1995).

[12] M. Tarek and D. J. Tobias, Phys. Rev. Lett. **89**, 275501 (2002).

[13] S. W. Lovesey and P. Schofield, J. Phys. C **9**, 2843 (1976).

[14] J. E. Boyd, A. Briskman, V. L. Colvin, and D. M. Mittleman, Phys. Rev. Lett. **87**, 147401 (2001).

[15] K. A. Mauritz and R. B. Moore, Chem. Rev. (Washington, D.C.) **104**, 4535 (2004), and references therein.

[16] S. Nemat-Nasser and J. Yu Li, J. Appl. Phys. **87**, 3321 (2000).

[17] X. Ye and M. Douglas Levan, J. Membr. Sci. **221**, 147 (2003).

[18] M. Saito, K. Hayamizu, and T. Okada, J. Phys. Chem. B **109**, 3112 (2005).
[19] A.-L. Rollet, O. Diat, and G. Gebel, J. Phys. Chem. B **106**, 3033 (2002), and references therein.
[20] C. Stone and A. E. Morrison, Solid State Ionics **152-153**, 1 (2002).
[21] G. Gebel, Polymer **41**, 5829 (2000).
[22] G. Gebel and O. Diat, Fuel Cells **5**, 261 (2005).
[23] A. Paciaroni, M. Casciola, E. Cornicchi, M. Marconi, G. Onori, M. Pica, and R. Narducci, J. Phys. Chem. B **110**, 13769 (2006).
[24] M.-C. Bellissent-Funel, J. Teixeira, S. H. Chen, B. Dorner, H. D. Middendorf, and H. L. Crespi, Biophys. J. **56**, 713 (1989).
[25] O. Plantevin, H. R. Glyde, B. Fråk, J. Bossy, F. Albergamo, N. Mulders, and H. Schober, Phys. Rev. B **65**, 224505 (2002).
[26] C. Mondelli, M. A. Gonzalez, F. Albergamo, C. Carbajo, M. J. Torralvo, E. Enciso, F. J. Bermejo, R. Fernandez-Perea, C. Cabrillo, V. Leon, and M. L. Saboungi, Phys. Rev. B **73**, 094206 (2006).
[27] D. S. Sivia, *Data Analysis: A Bayesian Tutorial* (Clarendon, Oxford, 2005).
[28] F. J. Bermejo, W. S. Howells, M. Jiménez-Ruiz, M. A. González, D. L. Price, M. L. Saboungi, and C. Cabrillo, Phys. Rev. B **69**, 174201 (2004).
[29] A. Orecchini, A. Paciaroni, A. De Francesco, L. Sani, M. Marconi, A. Laloni, E. Guarini, F. Formisano, C. Petrillo, and F. Sacchetti, Meas. Sci. Technol. **19**, 034026 (2008); A. Orecchini, A. Paciaroni, A. De Francesco, C. Petrillo, and F. Sacchetti, J. Am. Chem. Soc. **131**, 4664 (2009).
[30] Y. Xie, K. F. Ludwig, Jr., G. Morales, D. E. Hare, and C. M. Sorensen, Phys. Rev. Lett. **71**, 2050 (1993).